International Atomic Energy Agency

INDC(CSR)-010/GI
INT(86)-10

INDC INTERNATIONAL NUCLEAR DATA COMMITTEE

ANALYSIS OF NEUTRON INDUCED REACTIONS ON Ti ISOTOPES FROM 2 TO 20 MeV

S. Gmuca
Institute of Physics E.P.R.C.
Slovak Academy of Sciences
Dúbravska cestá 9, CS-842 28 Bratislava

October 1986

IAEA NUCLEAR DATA SECTION, WAGRAMERSTRASSE 5, A-1400 VIENNA

INDC(CSR)-010/GI
INT(86)-10

ANALYSIS OF NEUTRON INDUCED REACTIONS ON Ti ISOTOPES FROM 2 TO 20 MeV

S. Gmuca
Institute of Physics E.P.R.C.
Slovak Academy of Sciences
Dúbravska cestá 9, CS-842 28 Bratislava

October 1986

Reproduced by the IAEA in Austria
October 1986

86-04741

ANALYSIS OF NEUTRON INDUCED REACTIONS ON Ti ISOTOPES FROM 2 TO 20 MeV

Š. GMUCA
Institute of Physics E.P.R.C., Slovak Academy of Sciences, Dúbravská cesta 9, CS-842 28 Bratislava Czechoslovakia

Abstract

The Weisskopf-Ewing and preequilibrium models are used to obtain the cross sections of all the more important neutron threshold reactions on Ti isotopes. The calculated results are compared with the existing experimental data. The optical model is used for the calculation of reaction cross sections.

1. INTRODUCTION

The aim of this work is to present a complete and consistent analysis of the more important interactions of neutrons with Ti isotopes in the energy range 2-20 MeV.

The current phenomenological theory of nuclear reactions at intermediate and low energies /$E \lesssim 50$ MeV/ is based on various models of the reaction mechanism.

At lower excitation energies, most reactions leading to the particle emission are well described by the compound-nucleus evaporation model. The Hauser-Feschbach theory provides the most consistent method of calculating the cross section of that process. In the case of neglecting the angular momentum conservation it reduces to the much simpler Weisskopf-Ewing calculation.

At higher excitation energies /$E \gtrsim 15$ MeV/, however, the contribution from the preequilibrium mechanism becomes signi-

---

Work performed under IAEA Co-operative Research Programme on the "Measurement and Analysis of 14 MeV Neutron Nuclear Data needed for Fission and Fusion Reactor Technology" and Research Agreement No 3436/CF.

ficant and cannot be neglected anymore. The exciton model of preequilibrium decay has recently been widely used to describe that fraction of cross sections.

Thus, over the incident particle energy range considered, the reaction mechanism changes in character, and the integral cross sections and the emission spectra of reaction products can only be described using a combination of both the compound-nucleus and preequilibrium models. Apparently, the relative contributions of both competing mechanisms would vary according to the reaction conditions. Several papers /see e.g. Holub et al. 1980 and references therein/ have been published demonstrating that such an approach can properly describe particle emission spectra and excitation functions of reactions in the separate reaction channels.

In this paper, emphasis is put on a simultaneous analysis of many reaction channels involved in the interactions of neutrons with Ti isotopes, using a consistent set of parameters. Most of the calculations are compared with the available experimental data. At low energies the reactions (n,n'), (n,p) and (n,α) dominate, while at higher energies (n,2n), (n,pn), (n,n'p) and (n,nα) become also important. The remainining possible reactions, (n,3n), (n,2p) and those embracing the complex particles other than α, do not contribute appreciably below 20 MeV and so are excluded from consideration.

2. OPTICAL MODEL CALCULATIONS

Most modern theoretical nuclear data evaluations employ an optical model analysis using either a phenomenological or microscopically derived optical potential. The importance of this component to the evaluation is obvious as it provides not only the total, shape-elastic and reaction cross sections, but also the neutron and charged-particle transmission coefficients that are used in Hauser-Feschbach statistical theory calculations. An important feature of such consistent analyses is that they usually have to cover a very wide energy range; typically from 100 keV to 20 MeV or more.

The low energy transmission coefficients preserve their importance even at high incident energies in order to cor-

rectly calculate the multiparticle emission in the various reaction chains.

In this paper, the optical model calculations were made using the spherical optical model code SCAT2 by Bersillon /1981/. The global optical model parameters of Perey /1963/ for protons, and those of McFadden and Satchler /1966/ for α-particles, were used. The neutron optical model parameters for Sc and Ti isotopes are listed in Table 1, and the total cross sections obtained with these potentials are shown in Figs. 1 and 2, and compared with the experimental data of Foster and Glasgow /1971/. These comparisons confirm that these potentials give an adequate description of the experimental data.

3. STATISTICAL MODEL CALCULATIONS

All calculations were made by using the Weisskopf-Ewing evaporation model in combination with the precompound exciton model. Since the Weisskopf-Ewing model is well known and its description may be found in original papers /Weisskopf 1937, Weisskopf and Ewing 1940/, only the precompound exciton model used and relevant parameters are briefly described below.

A closed-form exciton - model expression for differential precompound cross sections is given by

$$d\sigma(\alpha,\beta)/d\varepsilon_\beta = \sigma_\alpha^{CN}(E_i) \sum_{\substack{n=n_0 \\ \Delta n=+2}}^{\bar{n}} W_\beta(n,E,\varepsilon_\beta)\, T(n,E) \qquad /1/$$

The emission of particles of type β of kinetic energy ε_β from an n-exciton state of the composite system at an exciton energy E, is propotional to the emission rate $W(n,E,\varepsilon_\beta)$ multiplied by the time T(n,E) the system spends in this particular state. The total probability for the emission of particles β with energy ε_β is obtained by summing up the contributions from all exciton states until the equilibrium is reached. $\sigma_\alpha^{CN}(E_i)$ is the cross section for the formation of the composite system by an incoming particle α of energy E_i. The emission rate

$W_\beta(n,E,\varepsilon_\beta)$ is given by the usual expression

$$W_\beta(m,E,\varepsilon_\beta)=\frac{2s_\beta+1}{\pi^2\hbar^3}\,d\mu_\beta\,\varepsilon_\beta\,\sigma_\beta^{INV}(\varepsilon_\beta)\,Q_\beta(p)\,\frac{\omega(p-p_\beta,h,E_H)}{\omega(p,h,E,E_H)} \qquad /2/$$

Here the proton-neutron distinguishibility factor $Q_\beta(p)$, as suggested by Kalbach /1977/, makes it possible to use the one-fermion density of exciton states. The Ericson state density $\omega(p,h,E,E_H)$ for a n-exciton state /n=p+h/ corrected for the Pauli principle and the finite depth of hole excitation, as determined by Běták and Dobeš /1976/, is given by

$$\omega(p,h,E,E,E_H)=\frac{g^n}{p!\,h!\,(n-1)!}\sum_{\ell=0}^{h}\binom{h}{\ell}(-1)^{\ell}\times \qquad /3/$$

$$\times\left(E-A_{p,h}-\ell E_H\right)^{n-1}\Theta\left(E-A_{p,h}-\ell E_H\right),$$

where $A_{p,h}$ is the correction factor due to the Pauli principle /Meneses 1983/

$$A_{p,h}=\frac{1}{g}\left\{ph-p(p+1)/4-h(h+1)/4\right\}, \qquad /4/$$

and E_H is the finite depth of hole excitation /Cmuca 1980/. In fact, the inclusion of the correction for the finite depth of hole excitation is the only major difference between the commonly used exciton model and that used in this work. Such a type of correction is in accord with the recent results of Wilkinson /1977/, who pointed out the dominating role of the nuclear surface in nuclear interactions. In terms of energy, this means that the depth of hole excitation is expected to be comparable with the strength of the effective residual interaction which is a few MeV. This may be compared with the total depth of the Fermi sea, i.e. several tens of MeV. Indeed, the recent evaluation of the equilibration of finite fermion systems by Wolschin /1981/ showed that, during the relaxation process, the occupation probabilities of only a small part of the nucleons below the Fermi energy /holes/ were changed substantially. The remaining part of nucleons continued to be inviolab-

le. The width of the energy region influenced by the equilibration was approximately equal to the thermodynamic temperature of the compound nucleus. Thus, the following relation, based on the arguments given above, was adopted for the evaluation of the effective finite depth of hole excitation /Gmuca 1982/

$$E_H = \sqrt{E/a}, \qquad /5/$$

a being the level density parameter of compound nucleus.

The time $T(n,E)$ that the composite system spends in an n-exciton state was evaluated by the closed-form expressions

$$T(n,E) = \tau_n(E) \prod_{\substack{i=n_0 \\ \Delta i=+2}}^{n-2} \lambda^+(i,E)\, \tau_i(E) \qquad /6/$$

$$\tau_n(E) = \left[\lambda^+(n,E) + \sum_{\gamma} \int_0^{\varepsilon_{\gamma max}} W_{\gamma}(n,E,\varepsilon_{\gamma})\, d\varepsilon_{\gamma}\right]^{-1}, \qquad /6a/$$

where $\lambda^+(n,E)$ is the transition rate forming n+2 - exciton state. The λ^+ transition rate is given by the "golden rule" as

$$\lambda^+(n,E) = \frac{2\pi}{\hbar} |M|^2 \omega_f^+(n,E,E_H), \qquad /7/$$

where the density of accessible final states $\omega_f^+(n,E,E_H)$, corrected for the finite depth of hole excitation, was taken as given by Běták and Dobeš /1976/. For the normalization of the absolute magnitude of the λ^+ transition rate, it is necessary to know the averaged squared matrix element $|M|^2$. Since no reliable microscopic calculations exist for the two-body interaction in the nucleus, a phenomenological expression for $|M|^2$ is usually used. In this work, $|M|^2$ is expected to behave approximately as /Gmuca 1982/

$$|M|^2 = K\, g^{-3}\, E_H^{-1}, \qquad /8/$$

where the finite depth of hole excitation was taken into account. The single particle density g is related to the level

density parameter a by

$$g = \frac{6}{\pi^2} a \qquad /9/$$

The dimensionless free parameter K was recently determined to be 0.30 for neutron induced reactions /Gmuca 1982/.

In Weisskopf-Ewing model calculations the level density formula of the traditional Fermi gas form

$$\rho(u) = \frac{\sqrt{\pi}}{12} \frac{\exp\left\{2\left[a(u-\delta)\right]^{1/2}\right\}}{a^{1/4}(u-\delta)^{5/4}} \qquad /10/$$

was used at higher excitation energies, joining smoothly to the constant temperature formula for excitation energies below 5 MeV.

The a and δ are the parameters of the level density formula, and their values used are listed in Table 2. They were taken mainly from Grimes et al. /1974 and 1978/, and slightly modified /if necessary/ to achieve fits to the excitation functions and particle emission spectra calculated. These modifications were mainly due to different sets of the optical model parameters used.

The γ-ray competition may exert a serious influence upon the particle emission, particularly around thresholds. In this work, the γ-ray transmission coefficients of the Brink-Axel giant dipole resonance form were used, with the parameters taken from the systematics

$$\begin{aligned} E_{GDR} &= 80\ A^{-1/3} \quad /\mathrm{MeV}/, \\ \Gamma_{GDR} &= 5 \quad /\mathrm{MeV}/, \\ \sigma_{GDR} &= 13\ A/\Gamma_{GDR} \quad /\mathrm{mb}/. \end{aligned} \qquad /11/$$

No attempts were made to calculate γ-ray spectra. The γ-ray emission serves only as a competitor to the particle emission thus improving the description of the excitation functions, mainly near the thresholds.

4. RESULTS AND COMPARISONS TO DATA

The calculations were performed using the program SPECTR-II /Gmuca 1984/ that handles a complex sequence of compound nuclei resulting from the neutron and proton emission chains in a single run. Neutrons, protons, alphas /or other complex particles/ and γ-rays are allowed to be emitted from each compound nucleus. In Fig. 3, an example of calculations for n+^{48}Ti cross sections obtained in a single run is shown. Below, the results of calculations will be compared to the available experimental data.

n + ^{46}Ti

Neutron activation cross sections data for the ^{46}Ti(n,p)^{46}Sc reaction are relatively abundant and they are complemented at 15 MeV by total proton emission spectra measured using the quadrupole spectrometer by Grimes et al. /1977/. While there was no problem to describe the proton emission spectra at 15 MeV /see Fig. 4/, a successful description of the excitation function was only possible by varying the level density parameter a of the residual nucleus ^{46}Sc with energy /a similar problem was also met in ^{47}Ti(n,n'p+pn)^{46}Sc reaction, leading to the same residual nucleus/. The energy dependent form of a as given by Maino and Menapace /1983/

$$a(u) = \tilde{a}(1 - e^{-\gamma u}) \qquad /12/$$

was, therefore, adopted for ^{46}Sc with $\tilde{a}$ = 5.85 and γ =0.43. In this, case, a reasonable agreement both with the experimental data and with the ENDF/B-V evaluation was achieved /see Fig. 5/.

The only datum for alpha-production cross sections on ^{46}Ti is that of 15 MeV neutron induced alpha-production, as measured by Grimes et al. /1977/. Our calculation of this reaction is compared to the experimental spectrum in Fig. 6.

The experimental data for the ^{46}Ti(n,2n)^{45}Ti reaction are both abundant and consistent, and well described by the calculation. The agreement near the threshold indicates a correct low-energy neutron transmission coefficients behaviour governed by the neutron optical potential parameters listed in Table 1.

n + ^{47}Ti

Only few measurements of ^{47}Ti(n,p)^{47}Sc cross sections were made at energies other than 14-15 MeV. At energies below 10 MeV, mutually consistent data by Smith and Meadows /1975/, Swinhoe and Uttley /1979/ and Husain and Hunt /1983/ are available, and our calculations are fairly consistent with these/being only somewhat lower at energies below 5 MeV/, and with the ENDF/B-V evaluation. This is documented by Fig. 7. Above 10 MeV, however, there is a considerable disagreement between our calculation and the ENDF/B-V evaluation which is, in fact, based only on one older measurement by Pai /1966/. Unfortunately, due to a large spread, the integral cross sections measured at 14-15 MeV energies do not allow a reliable normalization of the calculation and thus do not improve the situation in the upper part of the neutron energy range considered. Our calculation is compared to the 14-15 MeV single-point data in Fig. 8.

The calculation of the ^{47}Ti(n,n'p+pn)^{46}Sc reaction is compared with three available experimental data and with the ENDF/B-V evaluation in Fig. 9. The energy-dependent level density parameter a for the ^{46}Sc nucleus was used as discussed earlier.

n + ^{48}Ti

The ^{48}Ti nucleus is the most abundant and most important isotope of the Ti isotopic chain. Experimental and evaluated data for (n,p), (n,n'p+pn) and (n,α) reactions are available, and the calculations are compared to them.

Many measurements of ^{48}Ti(n,p)^{48}Sc cross sections were made, and these are complemented by a recent measurement of a proton production spectrum on ^{48}Ti with 15 MeV neutrons by Grimes et al. /1977/. Our calculations are compared to the total proton emission spectrum in Fig. 10, to experimental cross sections from near the threshold up to 20 MeV in Fig. 11, and to some recent single-point measurements around 14-15 MeV in Fig. 12. As one may see, an excellent fit to the proton emission spectrum was achieved. The description of the excitation function is generally good. In the region 6-12 MeV, however, our calculation is about 12 % higher than the ENDF/B-V

evaluation; it fits the data of Swinhoe and Uttley /1979/ measured at several energies between 6 and 14 MeV, rather than the cross sections of Smith and Meadows /1975/ on which the evaluation in this region is based. A similar situation appears also in the region 14-16 MeV, where the calculation is in agreement with accurate measurements by Vonach et al. /1968/, Ribanský and Gmuca /1983/ and Swinhoe and Uttley /1979/, while the ENDF/B-V evaluation is lower.

Measurements of the integral cross sections of the (n,α) reaction on ^{48}Ti are few and scattered. The recent measurement of the 15 MeV neutron-induced alpha production on ^{48}Ti have improved this situation considerably. Our calculations of the ^{48}Ti(n,α) cross section from threshold to 20 MeV are compared with the experimental activation cross sections in Fig. 13, and with the alpha-production spectrum at 15 MeV in Fig. 14.

Only four measurements are available for the ^{48}Ti(n,n'p+pn)^{47}Sc reaction. Our calculation is compared with these and with the ENDF/B-V evaluation in Fig. 15.

n + ^{49}Ti

The ^{49}Ti nucleus has not been included into the ENDF/B-V evaluation. The experimental data are available for ^{49}Ti(n,p)^{49}Sc and ^{49}Ti(n,n'p+pn)^{48}Sc reactions. In both cases the data are scanty and concentrated within the 14-15 MeV region, except for the old data by Pai /1966/ covering the 13.5-19.5 MeV region. No data are available for energies below 13 MeV. Our calculations are compared to the experimental data for the ^{49}Ti(n,p) reaction in Fig. 16, and for the ^{49}Ti(n,n'p+pn) reaction in Fig. 17. All the experimental data were obtained using the activation method. Note that for the ^{49}Ti(n,p)^{49}Sc reaction no γ's are available for identification and counting of the reaction product and, therefore, β-counting had to be used. Probably this fact, in view of well known drawbacks of such a kind of counting, is responsible for the substantial inconsistency of measured cross sections in the 14-15 MeV region.

n + ^{50}Ti

The ^{50}Ti(n,p)^{50}Sc reaction has not been included into the ENDF/B-V evaluation. The calculation of the excitation function

of this reaction is compared to the experimental data in Fig. 18. Our results agree well with the data of Pai /1966/, Barreira and Fanger /1981/ and Ribanský and Gmuca /1983/. Those of Qaim and Molla /1977/, Schwerer et al. /1976/ and Viennot et al. /1981/ are somewhat lower, although giving a similar slope in the 14-15 MeV region. No data are available below 13 MeV.

The experimental cross sections for the $^{50}Ti(n,\alpha)^{47}Ca$ reaction are available at 14-15 MeV energies only. All data are mutually consistent within the error limits quoted, and well described by both the ENDF/B-V evaluation and our calculation as shown in Figs. 19,20 with seemingly somewhat preferable fit of the latter. At other energies, however, there is a strong disagreement between the evaluation and our calculation. Clearly, the experimental data at other /mainly higher/ energies are required to resolve this discrepancy.

5. CONCLUSION

The results presented in this paper show that most of neutron threshold reactions on Ti isotopes may be reliably described by a combination of Weisskopf-Ewing and preequilibrium models. In a few cases, however, there are a large discrepancies between our calculations and the ENDF/B-V evaluations. The most pronounced one is that of the $^{47}Ti(n,p)^{47}Sc$ reaction. Our calculation of the $^{47}Ti(n,p)^{47}Sc$ cross sections greatly overestimates the ENDF/B-V evaluation above 10 MeV. In this case, the Hauser-Feschbach calculation with a detailed gamma-ray cascade will be valuable.

The figures show only those cross sections that can be compared with existing experimental data. Numerical values of all the reactions calculated including total particle production cross sections may be obtained from the author upon request.

TABLE 1: Neutron optical potential parameters

Sc isotopes +)	r(fm)	a(fm)
$V_R(E) = 58.28 - 0.2189\ E - 24(N-Z)/A$	1.16	0.677
$W_D(E) = 9.765 - 12(N-Z)/A$	1.288	0.310
$V_{SO}(E) = 6.874$	1.185	0.760
Ti isotopes		
$V_R(E) = 48.979 - 0.2361\ E - 24(N-Z)/A$	1.287	0.560
$W_D(E) = 8.582 - 0.1074\ E - 12(N-Z)/A$	1.345	0.470
$W_V(E) = 0.718 + 0.1855\ E - 12(N-Z)/A$	1.345	0.470
$V_{SO}(E) = 6.2$	1.120	0.470

+) Based on the potential of Oka et al. (1982) for ^{45}Sc.

TABLE 2: Level density parameters

Nucleus	a(MeV^{-1})	δ(MeV)	Nucleus	a(MeV^{-1})	δ(MeV)
^{45}Ti	5.80	0.30	^{42}Ca	5.50	1.20
^{46}Ti	5.85	1.80	^{43}Ca	5.50	-1.00
^{47}Ti	5.90	0.00	^{44}Ca	5.85	1.40
^{48}Ti	5.80	1.80	^{45}Ca	5.80	-0.60
^{49}Ti	5.90	1.00	^{46}Ca	5.85	1.80
^{50}Ti	6.20	1.80	^{47}Ca	5.90	-1.20
^{51}Ti	6.30	0.60	^{48}Ca	5.80	1.80
^{45}Sc	5.80	0.00	^{49}Ca	5.90	1.00
^{46}Sc	5.85+)	-1.80	^{42}K	5.50	-1.60
^{47}Sc	5.90	0.20	^{43}K	5.80	0.00
^{48}Sc	5.90	-0.30	^{44}K	5.85	-1.40
^{49}Sc	6.20	1.80	^{45}K	5.90	0.00
^{50}Sc	6.20	-1.30	^{46}K	5.90	-1.60

+) The excitation energy dependent parameter (see text)

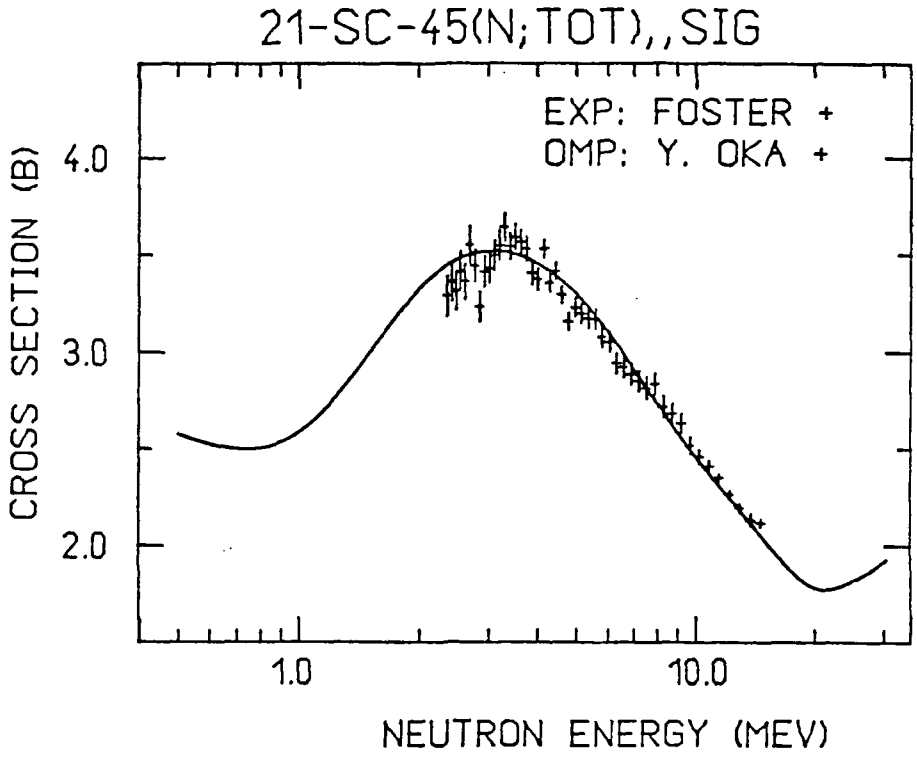

Fig. 1: Calculated and experimental values for n + ^{45}Sc total cross section.

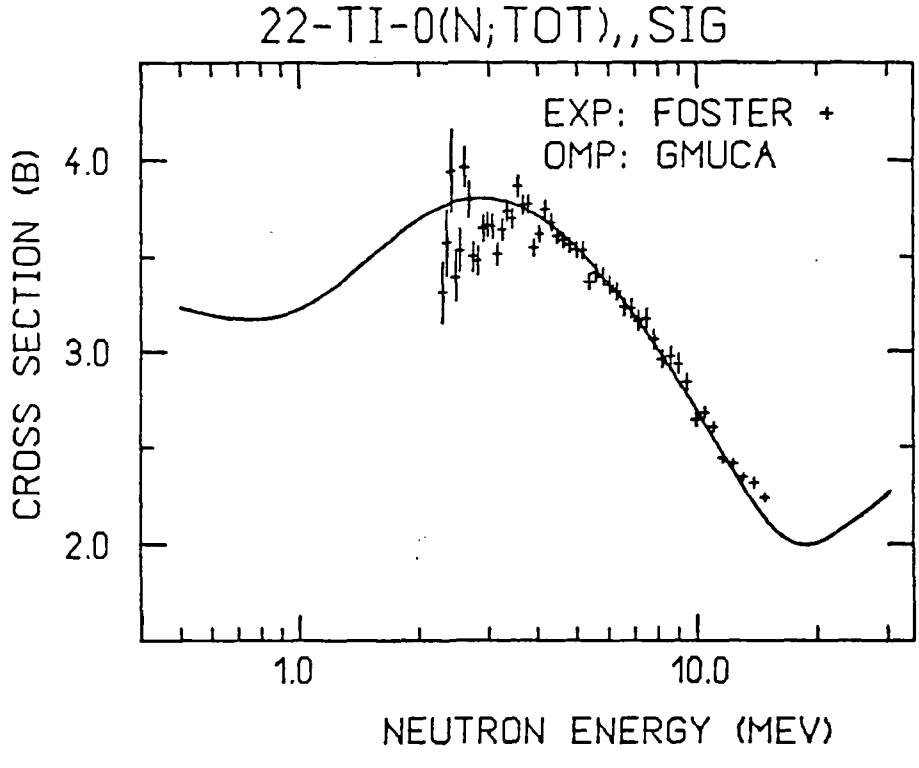

Fig. 2: Calculated and experimental values for n + Ti total cross section.

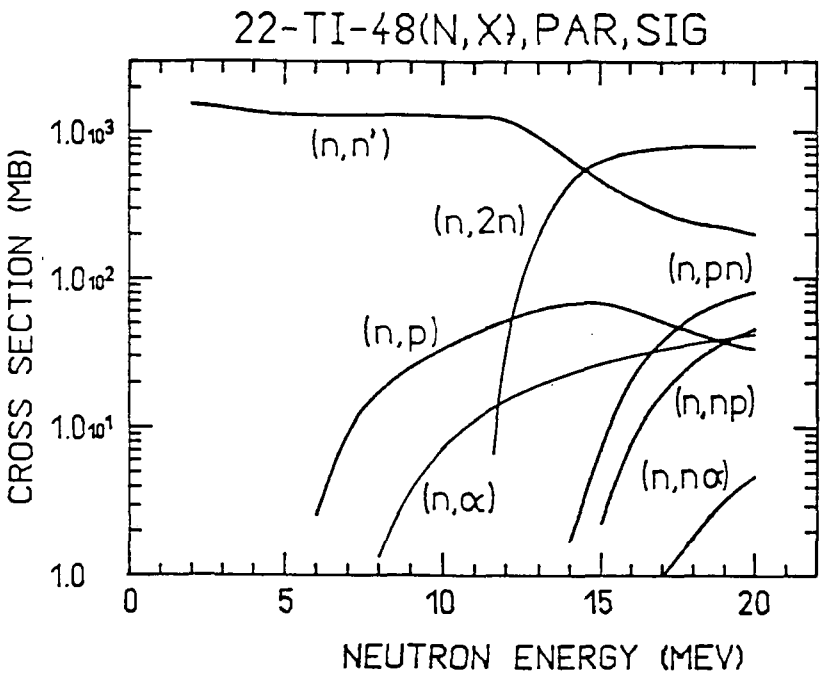

Fig. 3: Calculated reaction cross sections for n + ^{48}Ti interactions to 20 MeV.

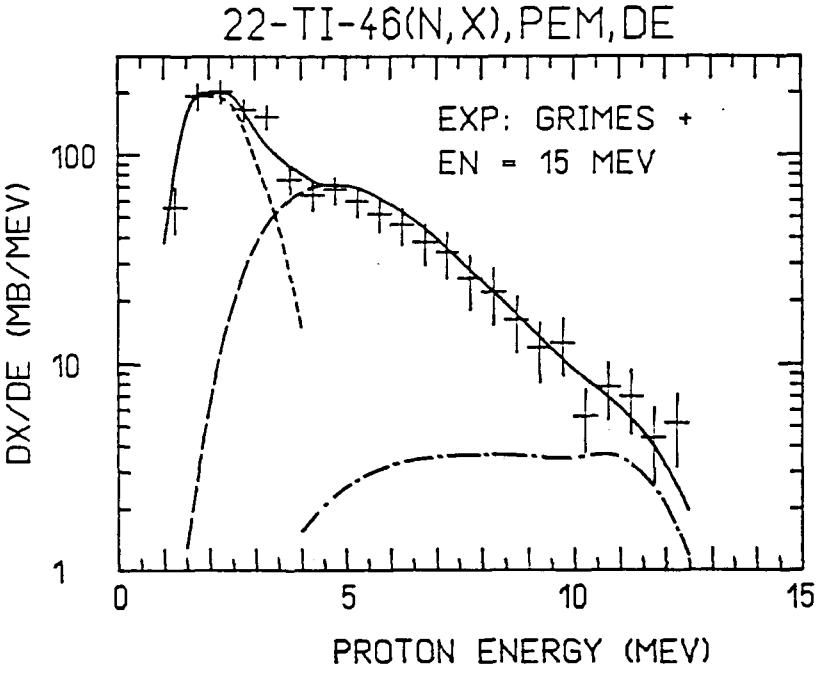

Fig. 4: Calculated and experimental proton emission spectra from 15 MeV neutron bombardment of ^{46}Ti. The solid curve is the total proton emission spectrum while the long-dashed and short-dashed curves represent contributions coming from (n,px) and (n,n'p) reactions. The dot-dashed curve is a preequilibrium part of the first proton emission spectrum.

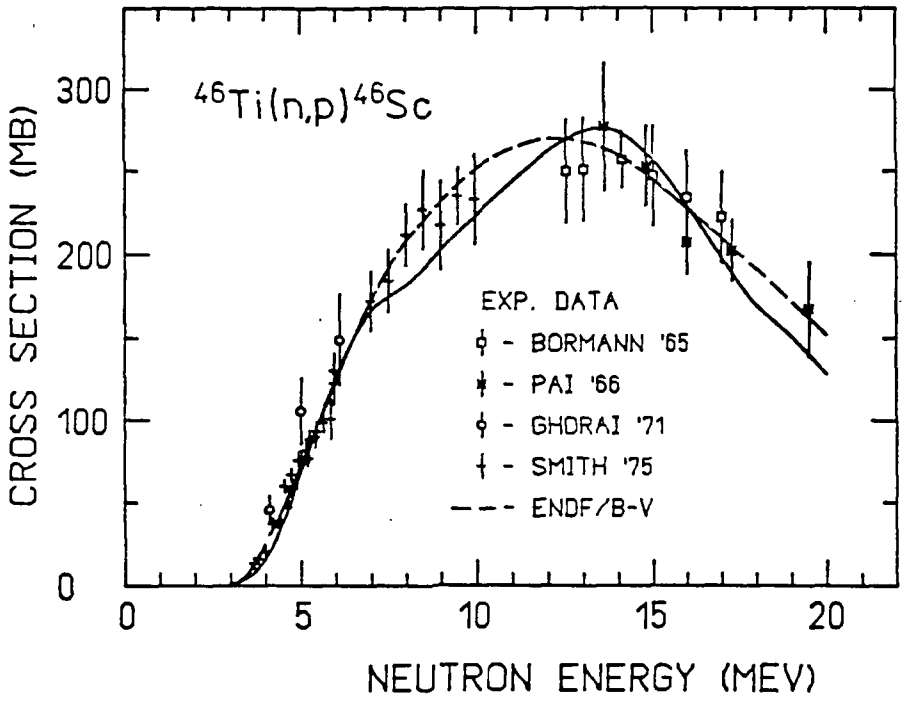

Fig. 5: Calculated and experimental cross sections for the $^{46}Ti(n,p)^{46}Sc$ reaction to 20 MeV. The dashed curve represents results of the ENDF/B-V evaluation.

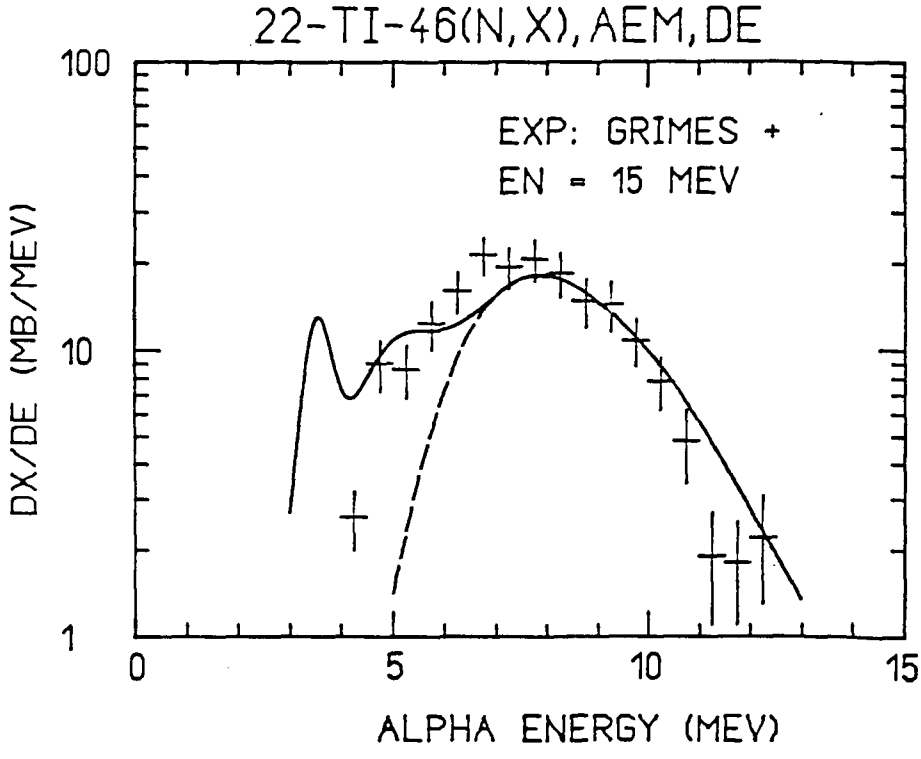

Fig. 6: Calculated and experimental alpha emission spectra from 15 MeV neutron bombardment of ^{46}Ti. The solid curve is the total alpha emission spectrum and the dashed curve represents the alpha spectrum from the first compound nucleus.

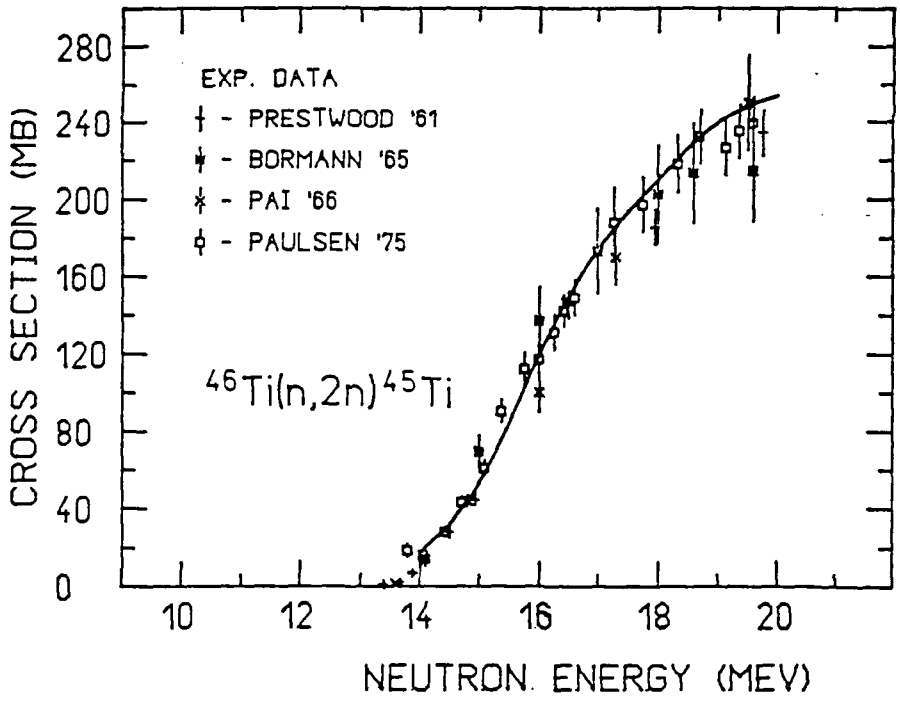

Fig. 6b: Calculated and experimental cross sections for the $^{46}Ti(n,2n)^{45}Ti$ reaction to 20 MeV.

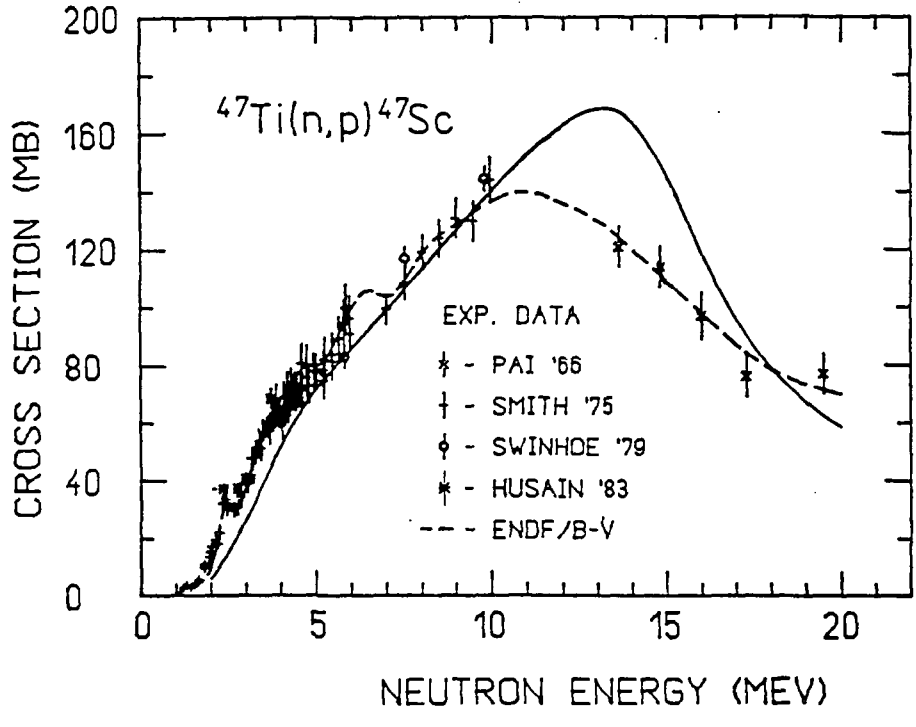

Fig. 7: Same as Fig. 5 for the $^{47}Ti(n,p)^{47}Sc$ reaction.

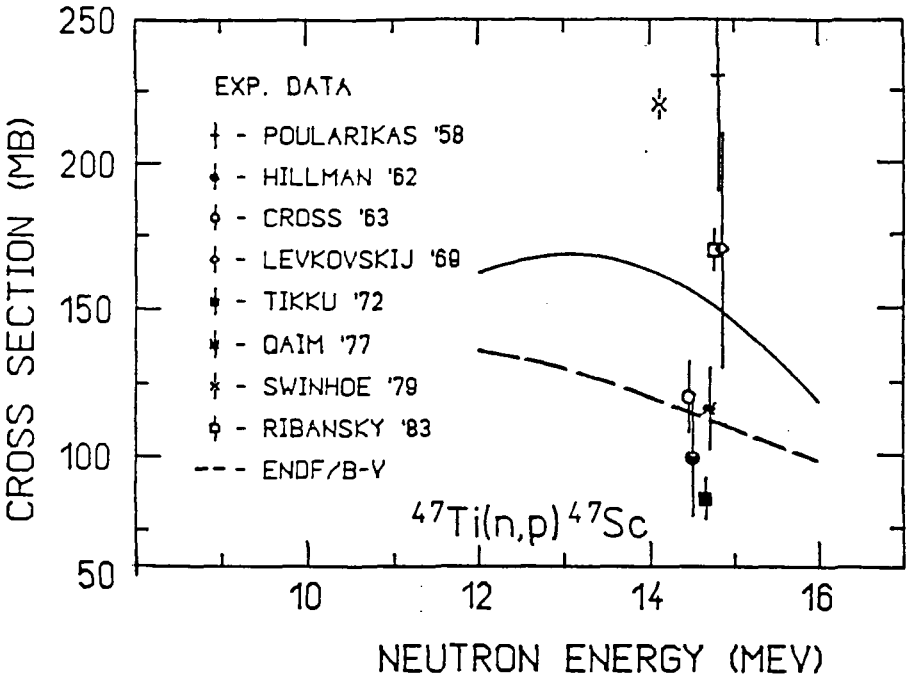

Fig. 8: A comparison of calculated cross sections (solid curve) for the $^{47}Ti(n,p)^{47}Sc$ reaction to single-point data around the 14-15 MeV region.

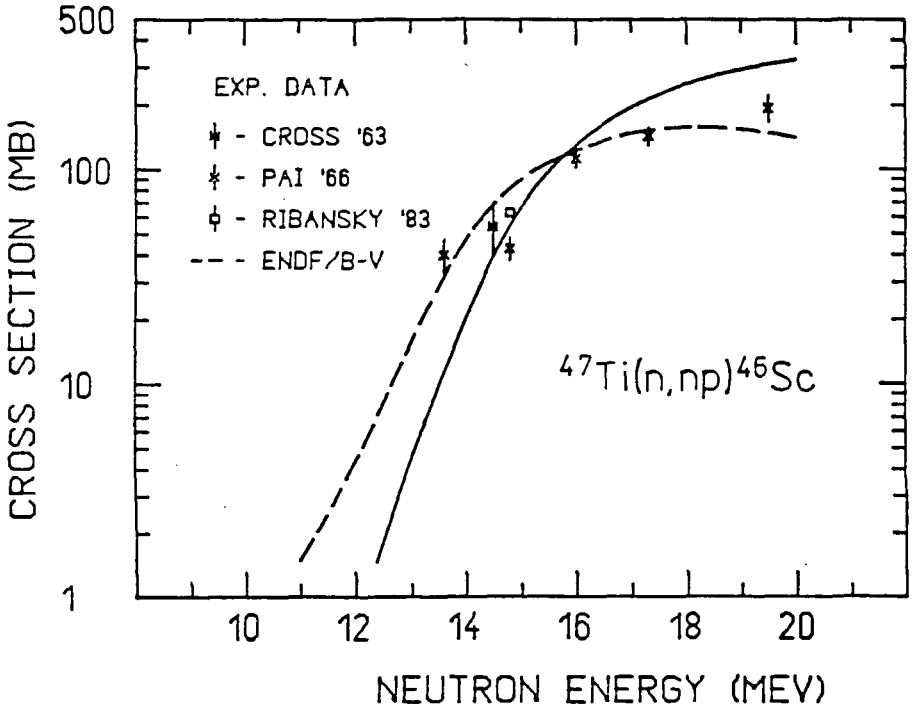

Fig. 9: Same as Fig. 5 for the $^{47}Ti(n,np)^{46}Sc$ reaction.

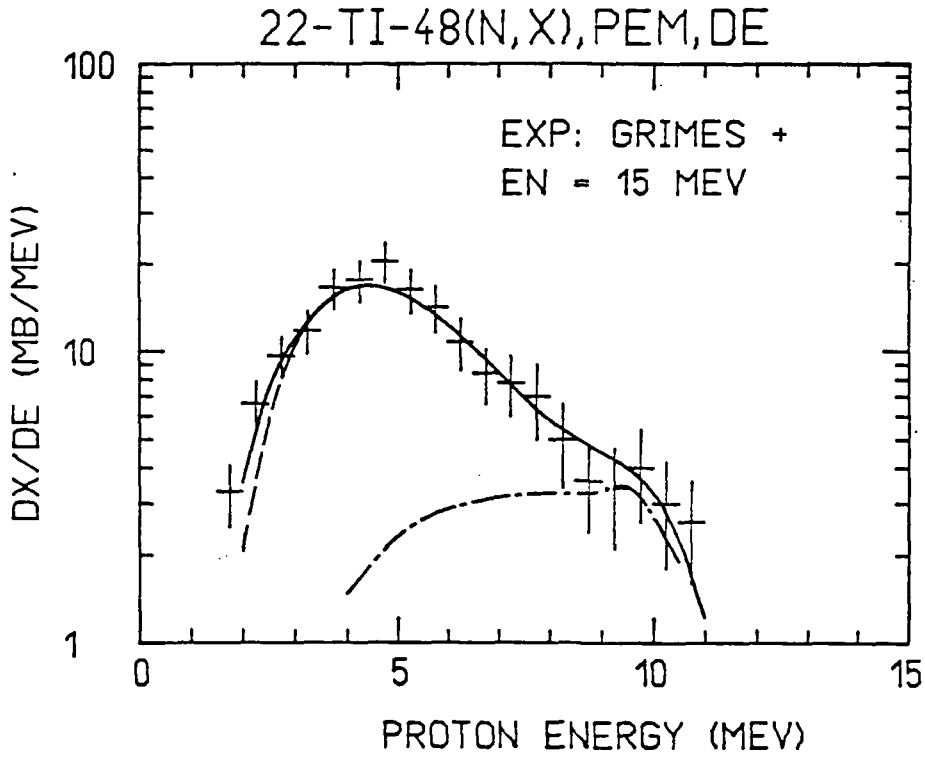

Fig. 10: Same as Fig. 4 for the n + ^{48}Ti interactions.

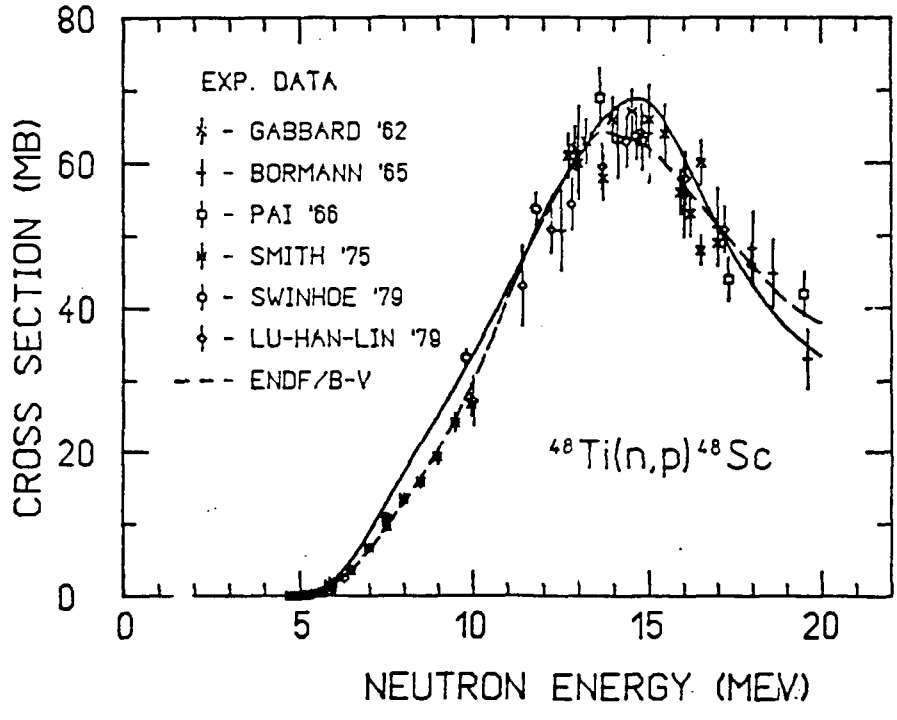

Fig. 11: Same as Fig. 5 for the ^{48}Ti(n,p)^{48}Sc reaction.

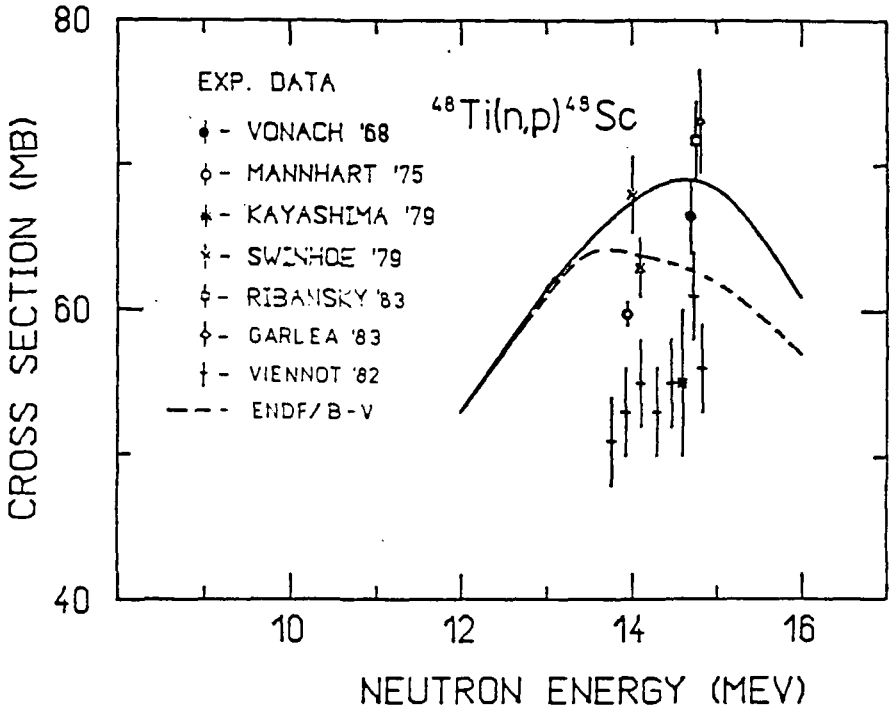

Fig. 12: Same as Fig. 8 for the $^{48}Ti(n,p)^{48}Sc$ reaction.

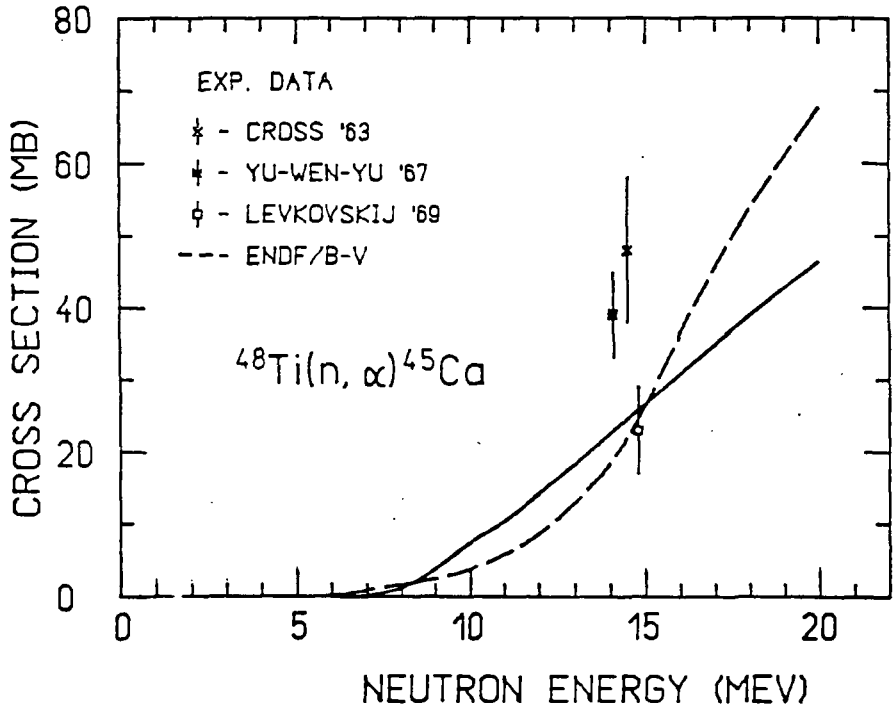

Fig. 13: Same as Fig. 5 for the $^{48}Ti(n,\alpha)^{45}Ca$ reaction.

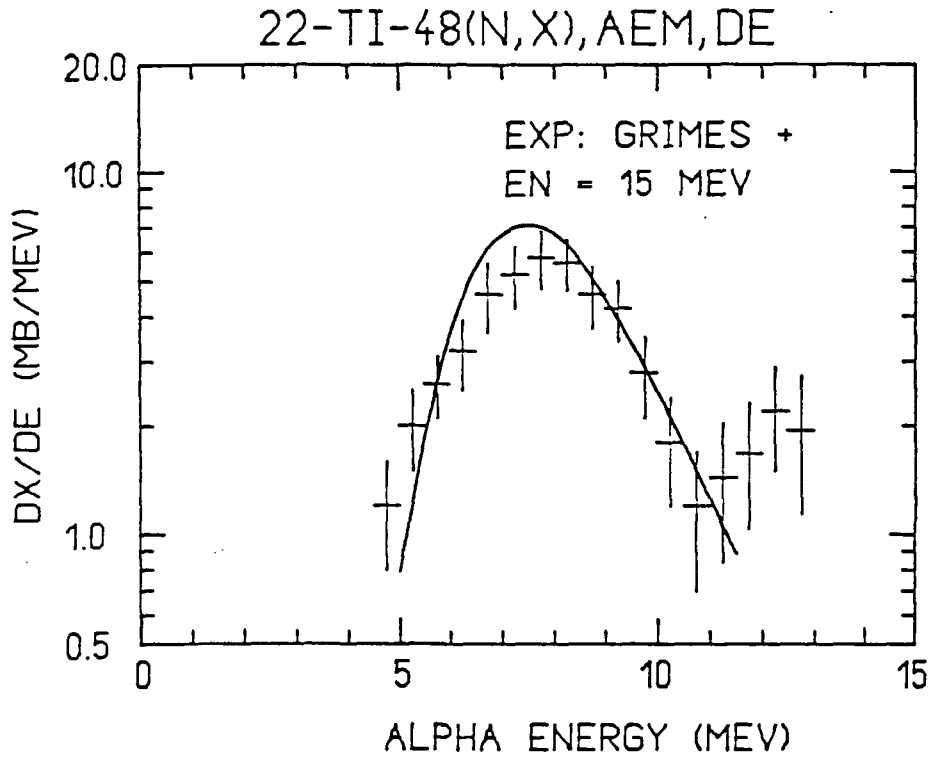

Fig. 14: Same as Fig. 6 for the n + ^{48}Ti interactions.

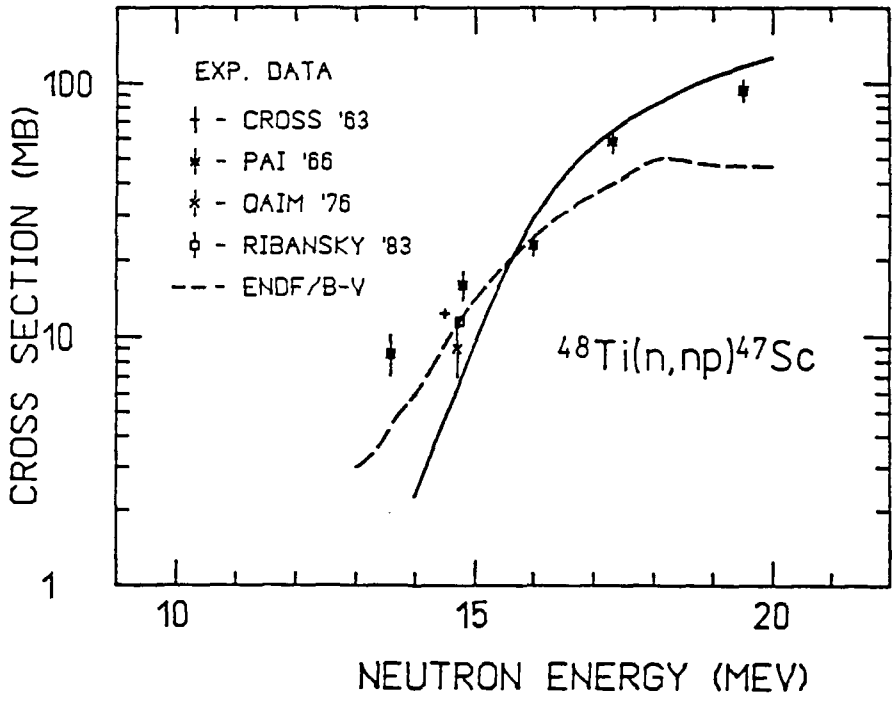

Fig. 15: Same as Fig. 5 for the ^{48}Ti(n,np)^{47}Sc reaction.

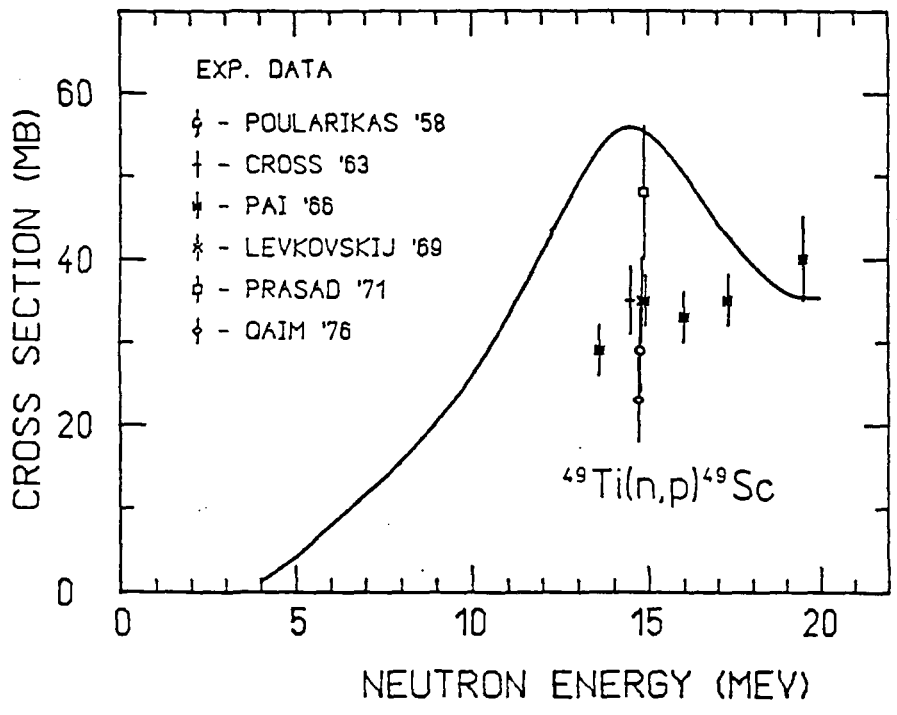

Fig. 16: Same as Fig. 5 for the ^{49}Ti(n,p)^{49}Sc reaction.

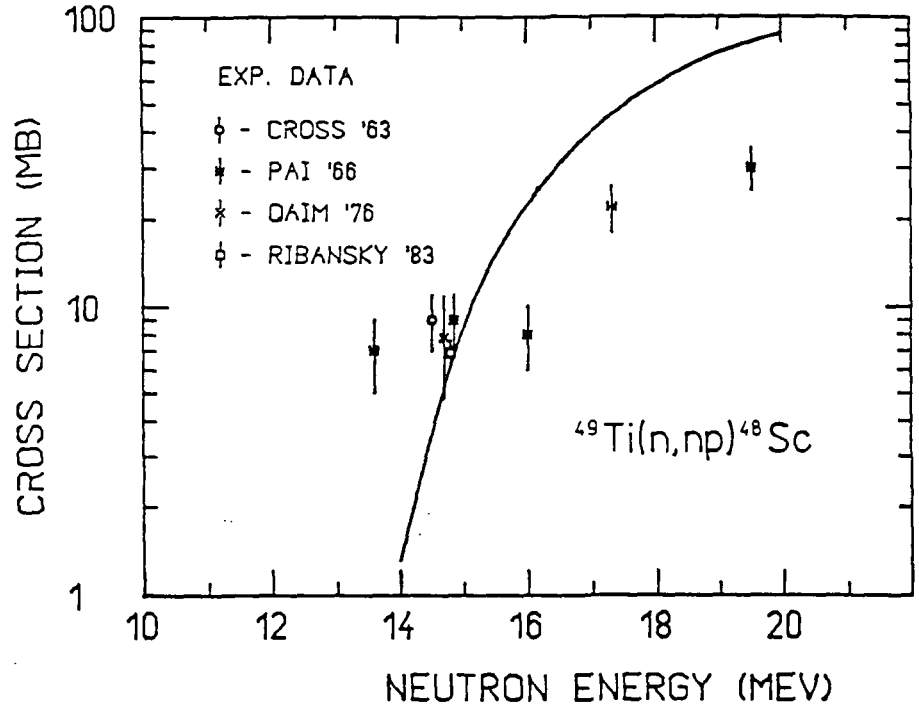

Fig. 17: Same as Fig. 5 for the ^{49}Ti(n,np)^{48}Sc reaction.

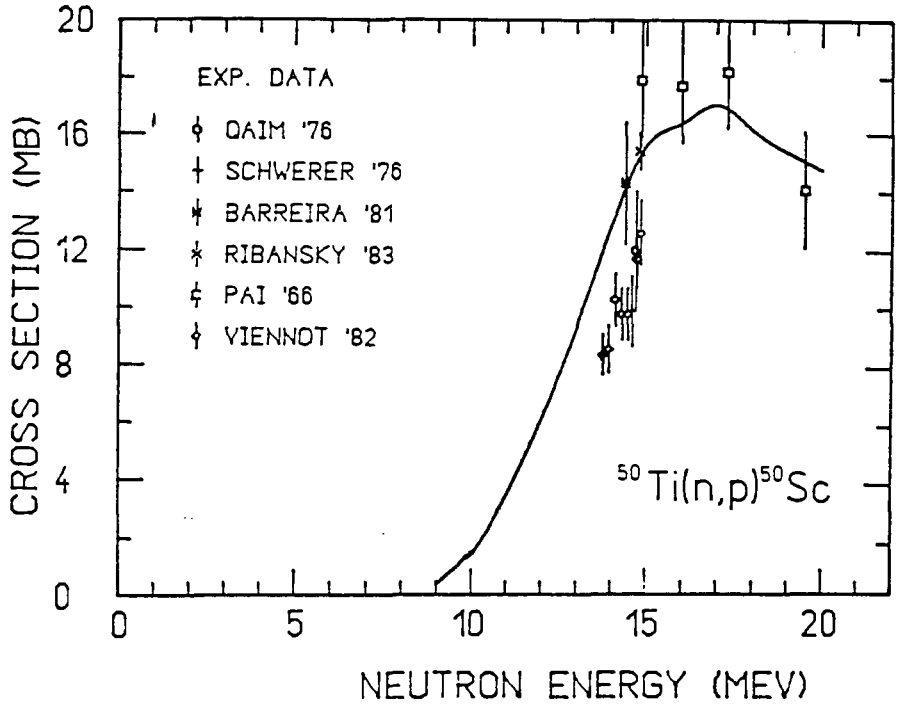

Fig. 18: Same as Fig. 5 for the $^{50}Ti(n,p)^{50}Sc$ reaction.

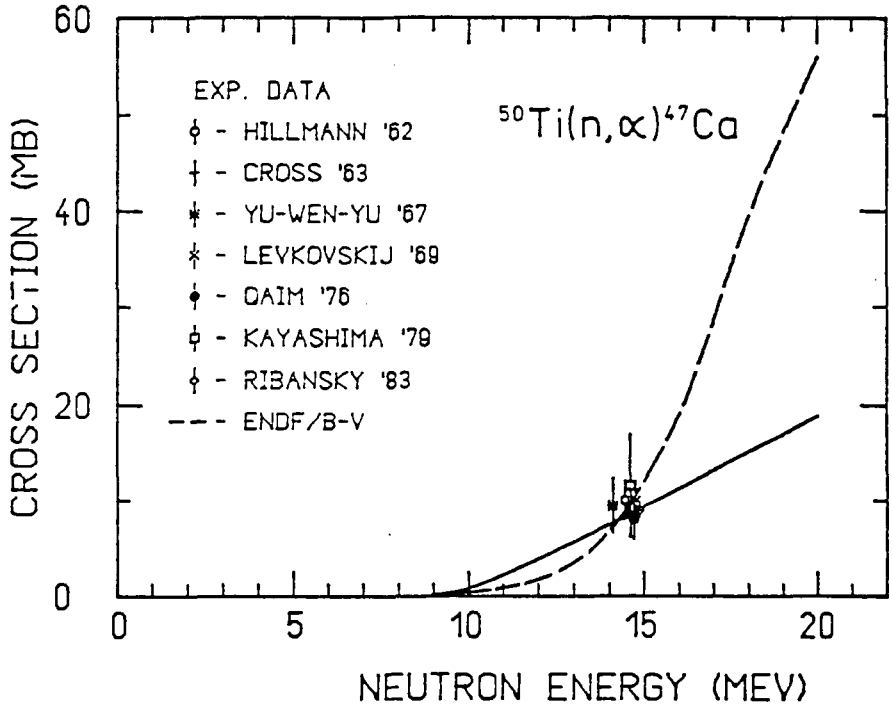

Fig. 19: Same as Fig. 5 for the $^{50}Ti(n,\alpha)^{47}Ca$ reaction.

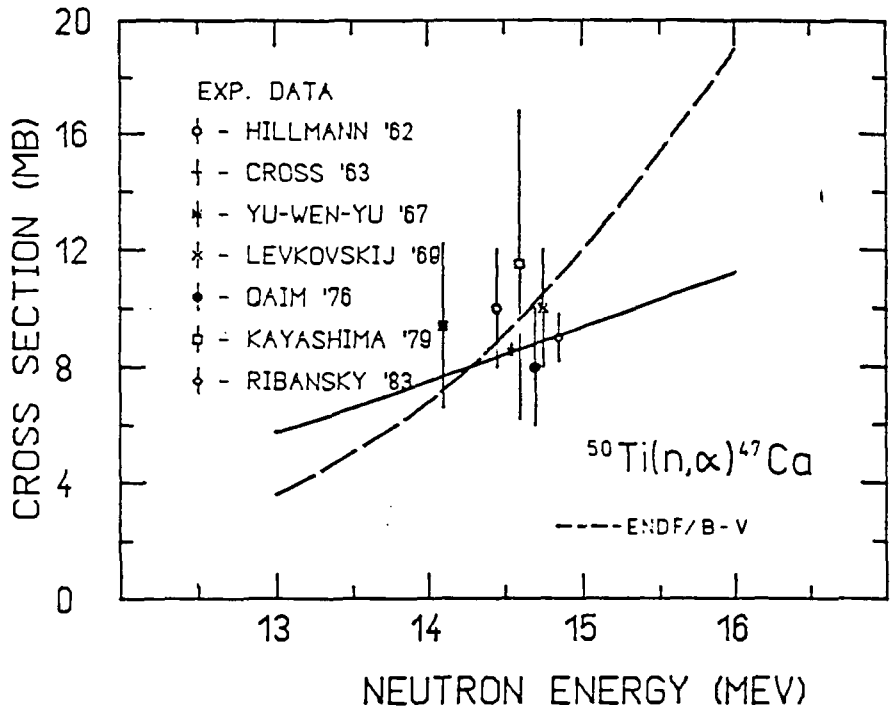

Fig. 20: Same as Fig. 8 for the $^{50}Ti(n,\alpha)^{47}Ca$ reaction.

REFERENCES

BARREIRA FILHO J.L. and FANGER H-.U., 1981, Data file EXFOR-21901 dated 1984-07-10, compare Report GKSS-81-E-53/1981/

BERSILLON O., 1981, SCAT2: Un programme de modele optique spherique, Report CEA-N-2227 (INDC(FR)-49/L)

BĚTÁK E. and DOBEŠ J., 1976, Z. Phys. A297/1976/319

BORMANN M. et al., 1965, Data file EXFOR-20887 dated 1980-12-18, compare Nucl. Phys. 63/1965/438

CROSS W.G. and PAI H.L., 1963, Data file EXFOR-11631 dated 1983-08-29, compare Report EANDC/CAN - 16/1963/p.1

FOSTER D.G. Jr. and GLASGOW D.W., 1971, Data file EXFOR-10047 dated 1982-10-19, compare Phys. Rev. C3/1971/576

GABBARD F. and KERN B.D., 1962, Data file EXFOR-11494 dated 1982-11-24, compare Phys. Rev. 128/1962/1276

GARLEA I. et al., 1983, Data file EXFOR-30804 dated 1984-07-06

GHORAI S.K. et al., 1971, Data file EXFOR-10180 dated 1982-09-15, compare J. Nucl. Energy 25/1971/319

GMUCA Š. and RIBANSKÝ I., 1980, In: Proc. 2nd Int. Symp. on Neutron Induced Reactions, Smolenice, June 25-29, 1979, eds., I. Ribanský and E. Běták, VEDA, Bratislava

GMUCA Š., 1982, Ph.D. thesis, Bratislava, unpublished

GMUCA Š., 1984, SPECTR-II: A statistical evaporation code with a precompound correction, Bratislava, unpublished

GRIMES S.M. et al., 1974, Phys. Rev. C10/1974/2373

GRIMES S.M. et al., 1977, Nucl. Sci. Eng. 62/1977/187

GRIMES S.M. et al., 1978, Phys. Rev. C17/1978/508

HILLMAN M., 1962, Data file EXFOR-11610 dated 1983-08-15, compare Nucl. Phys. 37/1962/78

HOLUB E. et al., 1980, Z. Phys. A296/1980/341

HUSAIN M.A. and HUNT S.E., 1983, Data file EXFOR-21879 dated 1984-02-02, compare Int. J. Radiat. Isotop. 34/1983/731

KALBACH C., 1977, Z. Phys. A283/1977/401

KAYASHIMA K. et al., 1979, Data file EXFOR-21300 dated 1984-01-06, compare Prog. Rept. NEANDC/J/-G1U/1979/p. 94

LEVKOVSKIJ V.N. et al., 1969, Data file EXFOR-40226 dated 1974-12-16, compare Sov. J. Nucl. Phys. 10/1969/44

LU-HAN-LIN et al., 1979, Data file EXFOR-30523 dated 1979-11-26, compare Phys. Energ. Fort. et Nucl. 3/1979/88 /in Chinese/

MAINO G. and MENAPACE E., 1983, In: Proc. IAEA Advisory Group Meeting on Basic and Applied Problems of Nuclear Level Densities, ed. M.R.Bhat, Upton, April 11-15, 1983, Report BNL-NCS-51694 /INDC/USA/-094/L

MANNHART W. and VONACH H., 1975, Data file EXFOR-20611 dated 1980-06-03, compare Z. Phys. A272/1975/279

MC FADDEN L. and SATCHLER G.R., 1966, Nucl. Phys. 84/1966/177

MENESES A.M.A., 1983, In: Proc. IAEA Advisory Group Meeting on Basic and Applied Problems of Nuclear Level Densities, Upton, April 11-15, 1983, Report BNL-NCS-51694 /INDC/USA/-094/L

OKA Y. et al., 1985, Evaluation of neutron nuclear data for ^{45}Sc. Report JAERI-M-9981 /INDC/JAP/-67/L

PAI M.L., 1966, Data file EXFOR-11630 dated 1983-08-15, compare Can. J. Phys. 44/1966/2337

PAULSEN A. et al., 1975, Data file EXFOR-20486 dated 1976-03-15, compare Atomkernenergie 26/1975/34

PEREY F.G., 1963, Phys. Rev. 131/1963/745

PRASAD R. and SARKAR D.C., 1971, Data file EXFOR-30336 dated 1981-02-04, compare Nuovo Cimento A3/1971/467

PRESTWOOD R.J. and BAYHURST B.P., 1961, Data file EXFOR-11645 dated 1983-08-29, compare Phys. Rev. 121/1961/1438

POULARIKAS A. and FINK R.W., 1959, Data file EXFOR-11484 dated 1982-11-24, compare Phys. Rev. 115/1959/989

RIBANSKÝ I. and GMUCA Š., 1983, Data file EXFOR-30660 dated 1983-06-29, compare J. Phys. G: Nucl. Phys.

SCHWERER O. et al., 1976, Data file EXFOR-20811 dated 1978-10-23, compare Anz. Oesterr. Akad. Wiss., Math.-Naturwiss. 113/1976/153

SMITH D.L. and MEADOWS J.W., 1975, Data file EXFOR-10238 dated 1982-10-15, compare Nucl. Sci. Eng. 58/1975/314, Reports ANL-NDM-10/1975/, ANL-NDM-13/1975

SWINHOE M.T. and UTTLEY C.A., 1979, Data file EXFOR-20986 dated 1981-07-22, compare Prog. Rept. AERE-PRINP-26/1979/p. 39

TIKKU U.K. et al., 1972, Data file EXFOR-30394 dated 1977-05-11, compare Proc. 15th Symp. Nucl. Solid State Physics, Chandigarh 1972, vol. 2, page 115

QAIM S.M. and MOLLA N.I., 1977, Datafile EXFOR-20721 dated 1980-10-15, compare Nucl. Phys. A283/1977/269

YU-WEN-YU and GARDNER D.G., 1967, Data file EXFOR-11583 dated 1983-08-15, compare Nucl. Phys. A98/1967/451

VIENNOT M. et al., 1981, Data file EXFOR-30627 dated 1982-06-03, compare Prog. Rept. MOH-4/1981/p.12

VONACH H.K. et al., 1968, Data file EXFOR-20815 dated 1980-06-03, compare Proc. Nucl. Cross-Sections Technol. Conf. Washington 1968, p. 885

WEISSKOPF V.F., 1937, Phys. Rev. 52/1937/295

WEISSKOPF V.F. and EWING D.H., 1940, Phys. Rev. 57/1940/472

WILKINSON D.H., 1977, Nucl. Instr. Meth. 146/1977/143

WOLSCHIN G., 1981, Report MPI-H-1981-V34, Heidelberg